

# Trajectory Control of Quadcopter by Designing Second Order SMC Controller

Mebaye Belete Mamo

Addis Ababa Science and Technology University, Ethiopia  
Mebaye.belete@aastu.edu.et

**Abstract** – This paper studies the modeling and control of quadcopter. It models the quadcopter nonlinear dynamics using Lagrange formalism and design controller for attitude (pitch & roll), heading & altitude tracking of the quadrotor. Mathematical modeling includes aerodynamic effects and gyroscopic moments. One Non-linear Control strategy, Second-Order Sliding Mode Control (SOSMC), based on a supertwisting algorithm has been proposed. The Controller has been implemented on the quadrotor physical model using Matlab/Simulink software. Finally, the performance of the proposed controller was demonstrated in the simulation study. The simulation results show excellent modeling and control performance.

**Keywords**-SOSMC; Lagrange; Mathematical Modelling; Quadrotor; MATLAB/Simulink

## I. INTRODUCTION

Quadrotor aerial vehicles are growing in increasing popularity in the fields of autonomous navigation, target tracking and surveillance, information gathering, and other high-level applications [1].

To perform tasks with high reliability, the quadrotor UAV requires good flight control capabilities. Therefore, the development of a specialized controller, which can take into account the quadrotor modeling nonlinearity with strongly coupled dynamics, underactuated characteristics, as well as parametric uncertainty, is always desired.

To ensure the stability of quadrotors, nonlinear, and robust controllers are often developed to reduce the effects of disturbances and uncertainties.

Going through the literature, one can see that most of the papers use two approaches for modeling the mechanical model. They are Newton-Euler and Newton-Lagrange but the most used one and it is most familiar and better in modeling is Newton-Euler [2, 3].

Linear adaptive methods such as model reference adaptive control have been suggested [4]. However, as for most linear methods, the achievable trajectory of the quadrotor is restricted due to the assumption of linearization. [5] proposed feedback controllers, which are based on a hierarchical control algorithm. The attitude is governed by employing a hybrid controller to overcome the well-known topological constraint, employed as a virtual input to stabilize the aircraft position, but still, there is a tracking problem.

For nonlinear control with unknown disturbance rejection, higher-order sliding mode control with active disturbance rejection based on nonlinear extended state observer [6-8] were designed. With this control scheme, higher-order SMC has shown effectiveness and accuracy in trajectory tracking.

Xu Zhou et al. [9] used both the PD controller and the sliding mode controller for the control of a quadrotor and showed that the sliding mode control exhibits efficiency, accuracy, and robustness than PD.

Considering fault-tolerant control (FTC), various nonlinear algorithms including backstepping, sliding mode, and adaptive FTC approaches for quadrotor attitude and altitude tracking can be found in [10], [11], and the references therein. However, in many existing works in the literature, backstepping controllers have only been developed for the position (i.e., outer-loop) control of quadrotors [12].

For indoor control of quadcopters different localization techniques can be employed, for example, the VICON motion capture system is one of the preferred systems for precise localization and it has been used widely in recent quadcopter studies [13, 14].

In summary, the literature on quadrotor control ignores the aerodynamic effect, air disturbance, and gyroscopic moment in the dynamic modeling of the quadrotor. Besides, in the case of sliding mode controller implementation, it does not reduce both the control effort and chattering effect.

The main contributions of this paper are summarized below in one paragraph.

This paper uses a novel approach to address the above problems. It designed a novel robust higher-order SMC controller with minimum control effort. It also shows the excellent effectiveness and accuracy of the designed controller using simulation and performance index measures.

The paper is organized into five sections. In section 1, it introduces the quadrotor UAV. In Section 2, it models the physical system by considering the aerodynamic and gyroscopic effects. In Section 3, it designs second-order SMC based on the supertwisting algorithm. In Section 4, it presents the simulation results obtained from the control implementation of the physical system in the Simulink environment. Finally, in Section 5, it presents the control effort and then concludes the work.

## II. MATHEMATICAL MODELLING

In this section, a mathematical model of Quadrotor UAV is established using the Lagrange formalism.

### A. Rotational Matrix

The orientation of the quadrotor is represented by Euler angles (pitch, roll, and yaw). To transform the body-fixed frame into the inertial frame; the z-y-x rotational matrix is considered [15].

To avoid system singularities, it is important to assume the angle bound.

$$-\frac{\pi}{2} < \varphi < \frac{\pi}{2}; -\frac{\pi}{2} < \theta < \frac{\pi}{2}; -\pi < \psi < \pi \quad (2.1)$$

$$\mathbf{R}_{(x,\varphi)} = \begin{pmatrix} 1 & 0 & 0 \\ 0 & c\varphi & -s\varphi \\ 0 & s\varphi & c\varphi \end{pmatrix} \quad \mathbf{R}_{(y,\theta)} = \begin{pmatrix} c\theta & 0 & s\theta \\ 0 & 1 & 0 \\ -s\theta & 0 & c\theta \end{pmatrix}$$

$$\mathbf{R}_{(z,\psi)} = \begin{pmatrix} c\psi & -s\psi & 0 \\ s\psi & c\psi & 0 \\ 0 & 0 & 1 \end{pmatrix} \quad (2.2)$$

Where  $c$  and  $s$  represent Cosine and Sine respectively.

Where  $\mathbf{R}_{(x,\varphi)}$ ,  $\mathbf{R}_{(y,\theta)}$  and  $\mathbf{R}_{(z,\psi)}$  represent rotation of rigid body in x, y and z-axis respectively.

The Euler rotation about z-y-x or  $\mathbf{R}_{xyz}$  is given by

$$\mathbf{R}_{xyz} = \mathbf{R}_{(z,\psi)} \mathbf{R}_{(y,\theta)} \mathbf{R}_{(x,\varphi)} \quad (2.3)$$

$$= \begin{pmatrix} c\psi c\theta & s\varphi s\theta c\psi - s\psi c\theta & c\varphi s\theta c\psi + s\psi s\varphi \\ s\psi c\theta & s\varphi s\theta s\psi + c\psi c\theta & c\varphi s\theta s\psi - s\psi c\varphi \\ -s\theta & s\varphi c\theta & c\varphi c\theta \end{pmatrix}$$

The model partitions naturally into translational and rotational coordinates [6]

$$\xi = (x, y, z) \in \mathbf{R}^3 \quad \eta = (\varphi, \theta, \psi) \in \mathbf{R}^3 \quad (2.4)$$

$\xi = (x, y, z)$  denotes the position vector of the center of mass of the Quadrotor relative to the fixed inertial frame and  $\eta = (\varphi, \theta, \psi)$  denotes the orientation of the quadrotor in the inertial frame. This is shown in Fig. 1 below

### B. Forces, Moments and Torques on Quadrotor

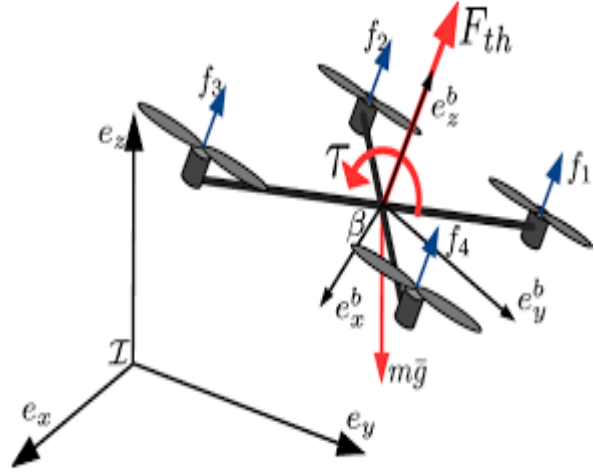
#### 1) Thrust Force

Quadrotor has four propellers so that it produces four thrust forces.

$$\mathbf{F} = \sum_{i=1}^4 \mathbf{F}_i \quad (2.5)$$

$$\mathbf{F} = \mathbf{F}_1 + \mathbf{F}_2 + \mathbf{F}_3 + \mathbf{F}_4 \quad (2.6)$$

Figure 1. Typical quadrotor schematic diagram with the body and inertial frames [16]



#### II) Moments

a) *Gyroscopic Moment*: There are two gyroscopic torques, this is due to the motion of the propeller (Mgp) and the quadrotor body (Mgb) [17] given by:

$$\mathbf{M}_{gp} = \sum_{i=1}^4 \Omega \wedge [0, 0, J_r (-1)^{i+1} \omega_i]^T \quad (2.7)$$

$$\mathbf{M}_{gb} = \Omega \wedge \mathbf{J} \Omega \quad (2.8)$$

$$\mathbf{J} = \begin{pmatrix} \mathbf{I}_{xx} & 0 & 0 \\ 0 & \mathbf{I}_{yy} & 0 \\ 0 & 0 & \mathbf{I}_{zz} \end{pmatrix} \quad (2.9)$$

Considering the quadrotor geometry is symmetric, all off-diagonal inertia matrix elements are zero.

$$\Omega = \begin{pmatrix} \dot{\varphi} \\ \dot{\theta} \\ \dot{\psi} \end{pmatrix}$$

b) *Aerodynamic friction moment*: the quadrotor moves in the air, due to this it is subjected to aerodynamic friction. The torque caused by this the aerodynamic friction is called aerodynamic friction moment. It is given by:

$$\mathbf{M}_a = \text{diag}(k_4, k_5, k_6) \begin{pmatrix} \dot{\varphi}^2 & \dot{\theta}^2 & \dot{\psi}^2 \end{pmatrix}^T \quad (2.10)$$

$\text{diag}(k_4, k_5, k_6)$  is the diagonal matrix of coefficients and  $\dot{\eta}^2$  is an angular velocity squared vector for rotational dynamics.

## III) Torques

## a) Pitch torque

It is proportional to the difference of the thrust force generated by the second and fourth propellers [18-20].

$$\tau_\phi = l(F_4 - F_2) \quad (2.11)$$

## b) Roll torque

It is proportional to the difference of the thrust force generated by the first and third propellers [7-9].

$$\tau_\theta = l(F_3 - F_1) \quad (2.12)$$

## c) Yaw torque

It is proportional to the difference of thrust force generated by all propellers [7-9].

$$\tau_\psi = c(F_1 - F_2 + F_3 - F_4) \quad (2.13)$$

## B. Modeling with Lagrange formalism

To obtain the quadrotor dynamics in terms of Lagrange, we use the Lagrange partial differential equation.

$$\frac{d}{dt} \frac{\partial L}{\partial \dot{q}} - \frac{\partial L}{\partial q} = F \quad (2.14)$$

Where  $F = (F_\xi, \tau)$ . We can calculate the translational and rotational components as follows

$$\mathbf{R}_{xyz} \begin{pmatrix} \mathbf{0} \\ \mathbf{0} \\ \sum_{i=1}^4 \mathbf{F}_i \end{pmatrix} - \begin{pmatrix} \mathbf{k}_1 \dot{\mathbf{x}} \\ \mathbf{k}_2 \dot{\mathbf{y}} \\ \mathbf{k}_3 \dot{\mathbf{z}} \end{pmatrix} = \mathbf{F}_\xi = \begin{pmatrix} (\mathbf{c}\phi\mathbf{s}\theta\mathbf{c}\psi + \mathbf{s}\psi\mathbf{s}\phi)\mathbf{u}_1 - \mathbf{k}_1 \dot{\mathbf{x}} \\ (\mathbf{c}\phi\mathbf{s}\theta\mathbf{s}\psi - \mathbf{s}\theta\mathbf{c}\psi)\mathbf{u}_1 - \mathbf{k}_2 \dot{\mathbf{y}} \\ (\mathbf{c}\phi\mathbf{c}\theta)\mathbf{u}_1 - \mathbf{k}_3 \dot{\mathbf{z}} \end{pmatrix} \quad (2.15)$$

$$\begin{pmatrix} \tau_\phi \\ \tau_\theta \\ \tau_\psi \end{pmatrix} - \mathbf{M}_a - \mathbf{M}_{gp} - \mathbf{M}_{gb} = \tau = \begin{pmatrix} \tau_\phi - \mathbf{J}_r \dot{\Omega}_r \dot{\theta} - (\mathbf{I}_{zz} - \mathbf{I}_{yy}) \dot{\theta} \dot{\psi} - \mathbf{k}_4 \dot{\phi}^2 \\ \tau_\theta + \mathbf{J}_r \dot{\Omega}_r \dot{\phi} - (\mathbf{I}_{xx} - \mathbf{I}_{zz}) \dot{\phi} \dot{\psi} - \mathbf{k}_5 \dot{\theta}^2 \\ \tau_\psi - (\mathbf{I}_{yy} - \mathbf{I}_{xx}) \dot{\theta} \dot{\phi} - \mathbf{k}_6 \dot{\psi}^2 \end{pmatrix} \quad (2.16)$$

Computing the Lagrange partial differential equation for all six generalized coordinates, get the following differential equations.

$$\ddot{\mathbf{x}} = (\mathbf{c}\phi\mathbf{s}\theta\mathbf{c}\psi + \mathbf{s}\psi\mathbf{s}\phi) \frac{\mathbf{u}_1}{\mathbf{m}} - \frac{\mathbf{k}_1}{\mathbf{m}} \dot{\mathbf{x}} \quad (2.17)$$

$$\ddot{\mathbf{y}} = (\mathbf{c}\phi\mathbf{s}\theta\mathbf{s}\psi - \mathbf{s}\theta\mathbf{c}\psi) \frac{\mathbf{u}_1}{\mathbf{m}} - \frac{\mathbf{k}_2}{\mathbf{m}} \dot{\mathbf{y}} \quad (2.18)$$

$$\ddot{\mathbf{z}} = (\mathbf{c}\phi\mathbf{c}\theta) \frac{\mathbf{u}_1}{\mathbf{m}} - \frac{\mathbf{k}_3}{\mathbf{m}} \dot{\mathbf{z}} - \mathbf{g} \quad (2.19)$$

$$\ddot{\phi} = \frac{\tau_\phi}{\mathbf{I}_{xx}} - \frac{\mathbf{J}_r \dot{\Omega}_r}{\mathbf{I}_{xx}} \dot{\theta} - \frac{(\mathbf{I}_{zz} - \mathbf{I}_{yy})}{\mathbf{I}_{xx}} \dot{\theta} \dot{\psi} - \frac{\mathbf{k}_4}{\mathbf{I}_{xx}} \dot{\phi}^2 \quad (2.20)$$

$$\ddot{\theta} = \frac{\tau_\theta}{\mathbf{I}_{yy}} + \frac{\mathbf{J}_r \dot{\Omega}_r}{\mathbf{I}_{yy}} \dot{\phi} - \frac{(\mathbf{I}_{xx} - \mathbf{I}_{zz})}{\mathbf{I}_{yy}} \dot{\phi} \dot{\psi} - \frac{\mathbf{k}_5}{\mathbf{I}_{yy}} \dot{\theta}^2 \quad (2.21)$$

$$\ddot{\psi} = \frac{\tau_\psi}{\mathbf{I}_{zz}} - \frac{(\mathbf{I}_{yy} - \mathbf{I}_{xx})}{\mathbf{I}_{zz}} \dot{\theta} \dot{\phi} - \frac{\mathbf{k}_6}{\mathbf{I}_{zz}} \dot{\psi}^2 \quad (2.22)$$

## III. CONTROL SYSTEM DESIGN

## A. Higher Order Sliding Mode Controller

## 1) Super-twisting algorithm

Consider once more the dynamical system of relative degree 1 and suppose that

$$\dot{\sigma} = \mathbf{h}(t, \mathbf{x}) + \mathbf{g}(t, \mathbf{x}) \mathbf{u} \quad (3.1)$$

Furthermore, assume that for some positive constants  $C, K_M, K_m, U_M, q$

$$\left| \dot{\mathbf{h}} + U_M \dot{\mathbf{g}} \right| \leq C, 0 \leq K_m \leq \mathbf{g}(t, \mathbf{x}) \leq K_M, \left| \frac{\mathbf{h}}{\mathbf{g}} \right| < q U_M, 0 < q < 1 \quad (3.2)$$

Then the control signal becomes

$$\mathbf{u} = -\lambda |\sigma|^{\frac{1}{2}} \text{sign}(\sigma) + \dot{\mathbf{u}} \quad \dot{\mathbf{u}} = \begin{cases} -\dot{\mathbf{u}}, & \text{for } |\mathbf{u}| > U_M \\ -a \text{sign}(\sigma), & \text{for } |\mathbf{u}| < U_M \end{cases} \quad (3.3)$$

**Theorem:** with  $K_m \alpha > C$  and  $\lambda$  sufficiently large, the controller (3.3) guarantees the appearance of a 2-sliding mode  $\sigma = \dot{\sigma} = 0$  in the system, which attracts the trajectories in finite time. The control  $\mathbf{u}$  enters in finite time segment  $[-U_M, U_M]$  and stays there. It never leaves the segment, if the initial value is inside at the beginning. For the theorem to be true, the sufficient condition is provided below

$$\lambda > \frac{\sqrt{\frac{2}{(K_m \alpha - C)(K_m \alpha + C)K_M(1+q)}}}{K_m^2(1-q)} \quad (3.4)$$

## a) Design of sliding mode control for altitude (z)

The state-space equation for altitude is as follows

$$\begin{aligned} \dot{\mathbf{x}}_5 &= \mathbf{x}_6 \\ \dot{\mathbf{x}}_6 &= (\mathbf{c}\phi\mathbf{c}\theta) \frac{\mathbf{u}_1}{\mathbf{m}} - \frac{\mathbf{k}_3}{\mathbf{m}} \mathbf{x}_6 - \mathbf{g} \end{aligned} \quad (3.5)$$

Then the linear sliding surface form as  $\sigma = \mathbf{c}\mathbf{e} + \dot{\mathbf{e}}$   $\mathbf{c} > 0$  it  $\mathbf{c}$  is larger the sliding dynamics decays rate is larger. Where  $\mathbf{c}$  is decay rate.

Where  $e = x_5^d - x_5$  and  $\dot{e} = \dot{x}_5^d - \dot{x}_5$ . By select  $c$  be 3, then the sliding surface become

$$\sigma = 3e + \dot{e} \quad (3.6)$$

Then computing  $\dot{\sigma}$  get

$$\dot{\sigma} = 3\dot{x}_5^d - \dot{x}_6 + \ddot{x}_5^d - (c\varphi c\theta) \frac{u_1}{m} + \frac{k_3}{m} x_6 + g \quad (3.7)$$

From the above 3.7, we assign

$$h(t, x) = 3\dot{x}_5^d - \dot{x}_6 + \ddot{x}_5^d + \frac{k_3}{m} x_6 + g \text{ and}$$

$$g(t, x) = -\frac{(c\varphi c\theta)}{m}$$

b) Design of sliding mode control for attitude (  $\varphi, \theta$  )

For  $\varphi$

The state-space equation for pitch is as follows

$$\begin{aligned} \dot{\mathbf{x}}_7 &= \mathbf{x}_8 \\ \dot{\mathbf{x}}_8 &= \mathbf{a}_1 \mathbf{u}_2 + \mathbf{a}_2 \bar{\Omega}_r \mathbf{x}_{10} + \mathbf{a}_3 \mathbf{x}_{10} \mathbf{x}_{12} - \mathbf{k}_4 \mathbf{a}_1 \mathbf{x}_8^2 \end{aligned} \quad (3.8)$$

Then the linear sliding surface form as  $\sigma = ce + \dot{e}$   $c > 0$  it  $c$  is larger the sliding dynamics decays rate is larger. Where  $c$  is decay rate.

Where  $e = x_7^d - x_7$  and  $\dot{e} = \dot{x}_7^d - \dot{x}_7$ . By select  $c$  be 3, then the sliding surface become

$$\sigma = 3e + \dot{e} \quad (3.9)$$

Then computing  $\dot{\sigma}$  get

$$\dot{\sigma} = 3\dot{x}_7^d - 3\dot{x}_8 + \ddot{x}_7^d - a_2 \bar{\Omega}_r x_{10} - a_3 x_{10} x_{12} + k_4 a_1 x_8^2 - a_1 u_2 \quad (3.10)$$

From the above equation, we assign

$$h(t, x) = 3\dot{x}_7^d - 3\dot{x}_8 + \ddot{x}_7^d - a_2 \bar{\Omega}_r x_{10} - a_3 x_{10} x_{12} + k_4 a_1 x_8^2$$

and  $g(t, x) = -a_1$

For  $\theta$

The state-space equation for the roll is as follows

$$\begin{aligned} \dot{\mathbf{x}}_9 &= \mathbf{x}_{10} \\ \dot{\mathbf{x}}_{10} &= \mathbf{a}_4 \mathbf{u}_3 + \mathbf{a}_5 \bar{\Omega}_r \mathbf{x}_8 + \mathbf{a}_6 \mathbf{x}_8 \mathbf{x}_{12} - \mathbf{k}_5 \mathbf{a}_4 \mathbf{x}_{10}^2 \end{aligned} \quad (3.11)$$

Then the linear sliding surface forms as

$\sigma = ce + \dot{e}$   $c > 0$  it  $c$  is larger, the sliding dynamics decay rate is larger. Where  $c$  is decay rate.

Where  $e = x_9^d - x_9$  and  $\dot{e} = \dot{x}_9^d - \dot{x}_9$ . By select  $c$  be 3, then the sliding surface become

$$\sigma = 3e + \dot{e} \quad (3.12)$$

Then computing  $\dot{\sigma}$  gets

$$\dot{\sigma} = 3\dot{x}_9^d - 3\dot{x}_{10} + \ddot{x}_9^d - a_5 \bar{\Omega}_r x_8 - a_6 x_8 x_{12} + k_5 a_4 x_{10}^2 - a_4 u_3 \quad (3.13)$$

From the above equation, we assign

$$h(t, x) = 3\dot{x}_9^d - 3\dot{x}_{10} + \ddot{x}_9^d - a_5 \bar{\Omega}_r x_8 - a_6 x_8 x_{12} + k_5 a_4 x_{10}^2$$

and  $g(t, x) = -a_4$

c) Design of sliding mode control for heading (  $\psi$  )

The state-space equation for yaw is as follows

$$\begin{aligned} \dot{\mathbf{x}}_{11} &= \mathbf{x}_{12} \\ \dot{\mathbf{x}}_{12} &= \mathbf{a}_8 \mathbf{x}_{10} \mathbf{x}_8 - \mathbf{k}_6 \mathbf{a}_7 \mathbf{x}_{12}^2 + \mathbf{a}_7 \mathbf{u}_4 \end{aligned} \quad (3.14)$$

Then the linear sliding surface forms as  $\sigma = ce + \dot{e}$   $c > 0$  it  $c$  is larger, the sliding dynamics decay rate is larger. Where  $c$  is decay rate.

Where  $e = x_{11}^d - x_{11}$  and  $\dot{e} = \dot{x}_{11}^d - \dot{x}_{11}$ . By selecting  $c$  be 3, then the sliding surface becomes

$$\sigma = 3e + \dot{e} \quad (3.15)$$

Then computing  $\dot{\sigma}$  we get

$$\dot{\sigma} = 3\dot{x}_{11}^d - 3\dot{x}_{12} + \ddot{x}_{11}^d - a_8 x_{10} x_8 + k_6 a_7 x_{12}^2 - a_7 u_4 \quad (3.16)$$

From the above equation, we assign

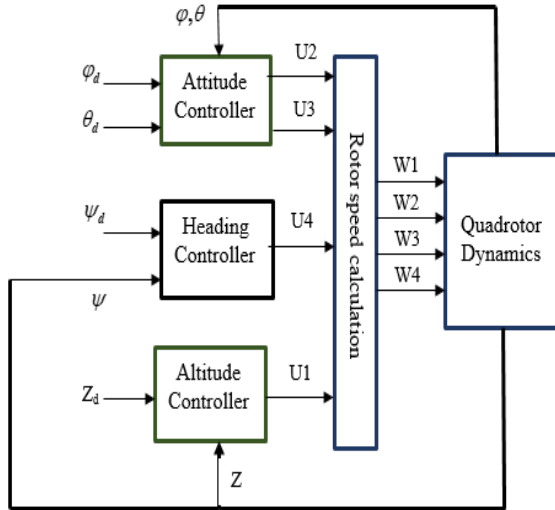
$$h(t, x) = 3\dot{x}_{11}^d - 3\dot{x}_{12} + \ddot{x}_{11}^d - a_8 x_{10} x_8 + k_6 a_7 x_{12}^2$$

and  $g(t, x) = -a_7$

## B. Designed Control System Scheme Block Diagram

A diagram of the proposed control approach can be seen in Fig. 2. The diagram clearly illustrates the Implementation of a control system designed on the quadrotor physical system.

Figure 2. Control system scheme block diagram



### C. Reference or Desired values for Tracking

$$\begin{cases} z_d = 0.5 + t \\ \varphi_d = 0.174 \sin(t) \\ \theta_d = 0.174 \sin(t) \\ \psi_d = 0.174 \sin(t) \end{cases} \quad (3.17)$$

### D. Calculated Controller Parameters for Tracking

The controller parameters listed below in Table I are calculated based on the above theorem.

TABLE I. REGULATION PROBLEM CONTROLLER PARAMETERS FOR SLIDING MODE CONTROL

| Variables/statuses | Calculated Values                |                                 |
|--------------------|----------------------------------|---------------------------------|
|                    | $\lambda$ for Super-twisting SMC | $\alpha$ for Super-twisting SMC |
| Z(altitude)        | 60                               | 1                               |
| Pitch(phi)         | 15                               | 5                               |
| Roll (theta)       | 15                               | 5                               |
| Yaw (psi)          | 5                                | 1                               |

## IV. SIMULATION RESULTS AND ANALYSIS

### A. Simulation Graphs and Analysis

In this section, numerical simulations are carried out on the quadrotor system to validate the control performance of the proposed sliding mode control. For simulation purposes, the parameters listed in Table II are used.

TABLE II. PHYSICAL PARAMETERS FOR THE QUADROTOR [17]

| Parameters  | Calculated Parameter                            |
|---|---|
|   | Values and Unit                                 |
| Arm Length(l)   | 0.5m  |
| Total mass  | 0.5 kg  |
| Quadrotor mass moment of inertia (I)                    | <b>diag</b> (0.005,0.005,0.01) kgm <sup>2</sup> |
| Motor inertia (Jr )                                     | $2.8385 \times 10^{-5}$ N.m/rad/s <sup>2</sup>  |
| Coefficient of Lift (b)                                 | $2.9 \times 10^{-5}$                            |
| Coefficient of Drag (d)                                 | $3 \times 10^{-7}$                              |
| Aerodynamic friction Coefficients (K <sub>1,2,3</sub> ) | 0.3729  |
| Translational drag Coefficients (K <sub>4,5,6</sub> )   | $5.56 \times 10^{-4}$                           |
| Gravitational acceleration(g)                           | 9.81 m/s <sup>2</sup>                           |

The overall results are shown in Fig. 3, Fig. 4, Fig. 5, and Fig. 6, respectively. Fig.3 demonstrates the tracking performance of altitude, which is shown that the response of the quadrotor can follow the desired value as closely. Fig. 4, Fig. 5, and Fig. 6 show the tracking performances of the three Euler angles, i.e., pitch, roll, and yaw, respectively. It shows that the quadrotor tracks the reference values for the three Euler angles as closely as possible with errors in the order of 0.001.

It can be seen from the above simulation results that the proposed third-order sliding mode control is effective and accurate.

Figure 3 Altitude tracking controller performance using Third-order SMC

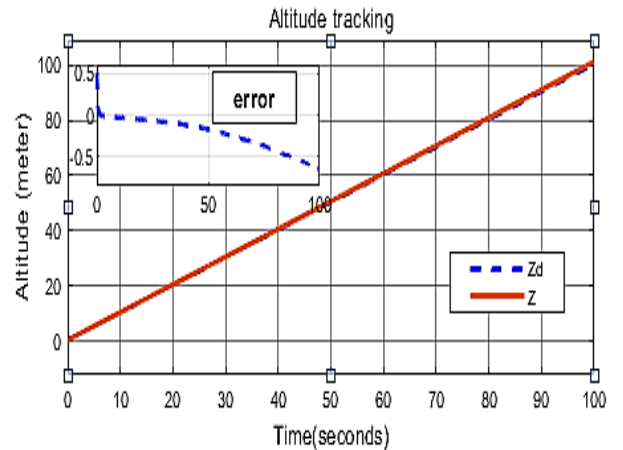


Figure 4. Pitch Tracking controller performance using Third-order SMC

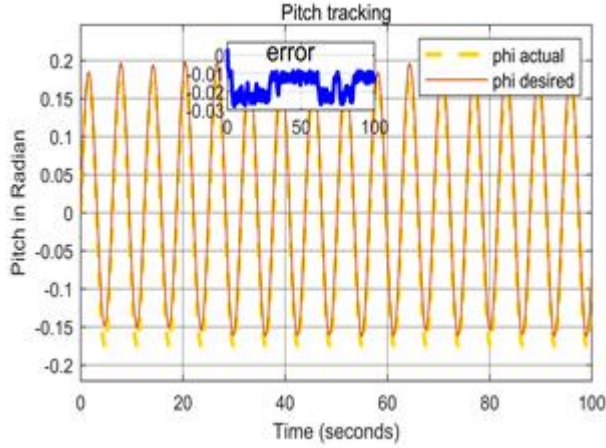


Figure 5. Roll tracking controller performance using Third-order SMC

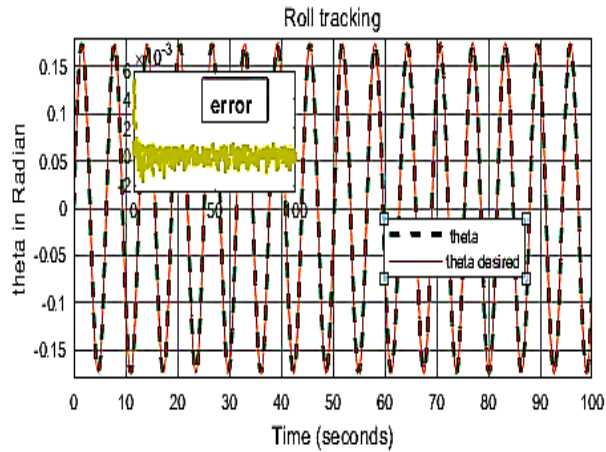
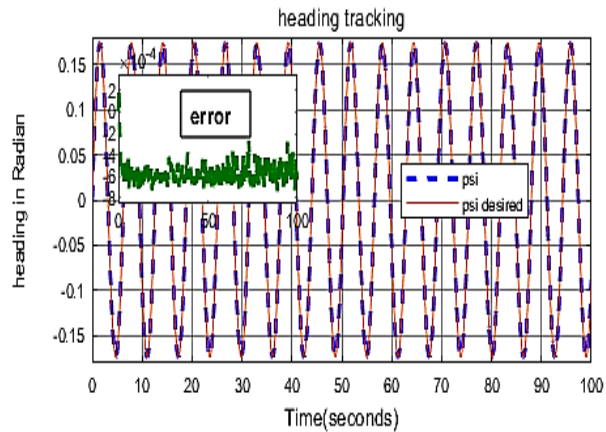


Figure 6. Yaw (heading) regulation controller performance using Third-order SMC



#### D. 3D tracking using second-order super twisting SMC

##### II. Regular helix tracking

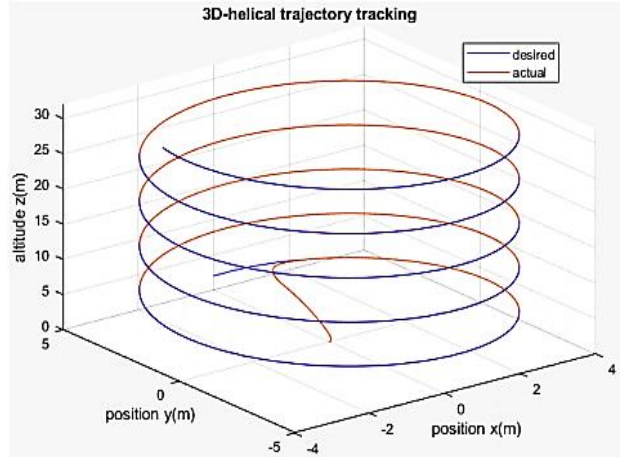
In this section, the regular helix tracking performance of the designed controller is demonstrated using three controlled variables. The variables are pitch, heading, and altitude. The variables selection among the four candidates is based on one from altitude, one from attitude, and one from heading. The desired trajectory is a regular helix generated from these parametric equations. The base of the regular helix is an ellipse.

$$\begin{cases} xd = \varphi_d = 4 \sin(t) \\ yd = \psi_d = 5 \cos(t) \\ zd = z_d = 2 + t \end{cases} \quad (3.18)$$

$xd$ ,  $yd$  and  $zd$  are the desired trajectories in the x-axis, y-axis, and z-axis respectively.

In Fig.7, the result shows the tracking controller performance of the designed pitch, heading, and altitude controller on three-dimensional space. As seen from the three-dimensional plot, the quadrotor has given a mission to track desired the three-dimensional trajectory indicated by the blue solid line described using the above parametric equations. As expected, the designed controllers for the three variables enable the quadrotor to track perfectly the desired three-dimensional trajectory.

Figure 7. 3D regular helical trajectory tracking using second-order SMC



##### III. Oblique helix tracking

In this section, the oblique helix tracking performance of the designed controller is demonstrated using the three controlled variables. The variables are roll, heading, and altitude. The variables selection among the four candidates is based on one from altitude, one from attitude, and one from heading. The desired trajectory is an oblique helix generated from the parametric equations below.

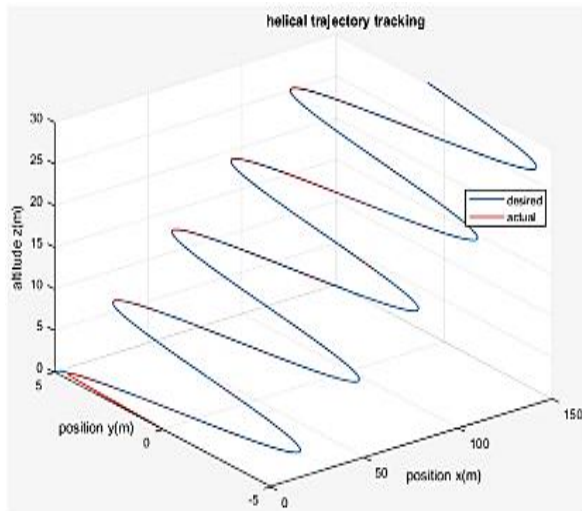
$$\begin{cases} xd = \theta_d = 5t \\ yd = \psi_d = 5 \cos(t) \\ zd = z_d = t \end{cases} \quad (3.19)$$

$xd$ ,  $yd$  and  $zd$  are the desired trajectories in the x-axis, y-axis, and z-axis respectively.

In Fig.8, the result shows the tracking controller performance of the designed roll, heading, and altitude controller on three-dimensional space. As seen from the three-dimensional plot, the quadrotor has given a mission

to track the desired three-dimensional trajectory indicated by the blue solid line described by the above parametric equations. As expected, the designed controllers for the three variables enable the quadrotor to track perfectly the desired three-dimensional trajectory.

Figure 8. 3D Oblique helical trajectory tracking using second-order SMC



#### E. Control Signals for Tracking using Second-order SMC

The control law is designed in the control system section using second-order SMC based on a super twisting algorithm. The quadrotor physical system contains four control inputs as seen from the dynamic modeling equations. The control inputs are  $U_1$ ,  $U_2$ ,  $U_3$ , and  $U_4$  respectively. The control effort liberated to track the desired trajectory depicted in equation (3.17) is shown below in Fig. 9, Fig. 10, Fig. 11, and Fig.12. The control simulation for pitch, roll, and yaw control signal is done by taking maximum amplitude of references input for the three Euler angles and give this as step signal for the quadrotor plant.

The control efforts are within the practical region and less than what is needed in a real-life scenario. Typical quadrotor motors can generate control signals with mild rotation (around 3000 rpm), so we can implement the designed controller algorithm in real-life application. Besides, the chattering effect is reduced to a greater extent to support this numerical value; the frequency of oscillation is from 0 to 10 Hz (0 to pitch control effort and 10 to altitude control effort). The rest two lies in between these values.

Figure 9. Altitude control signal for tracking

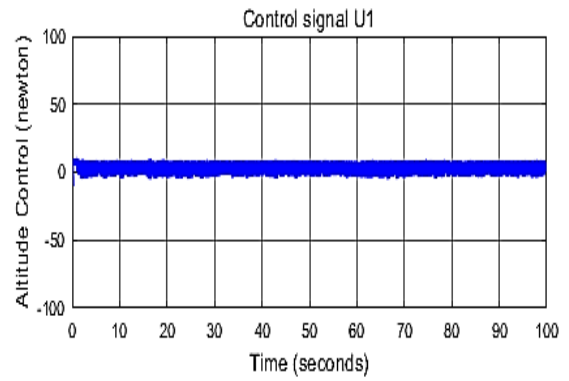


Figure 10. Pitch control signal for tracking

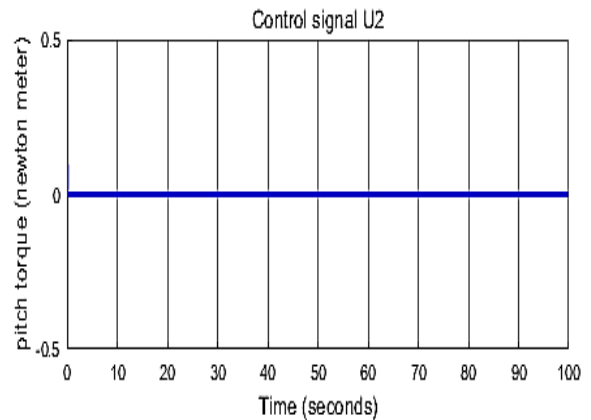


Figure 11. Roll control signal for tracking

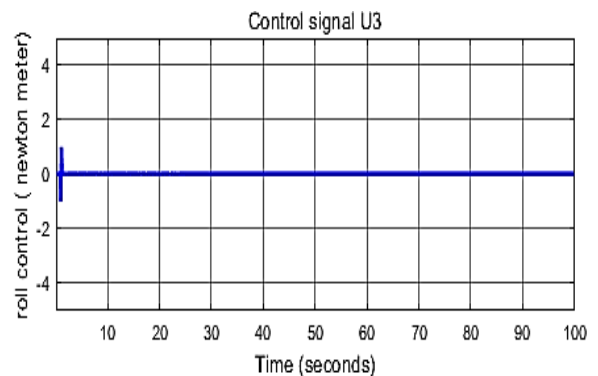
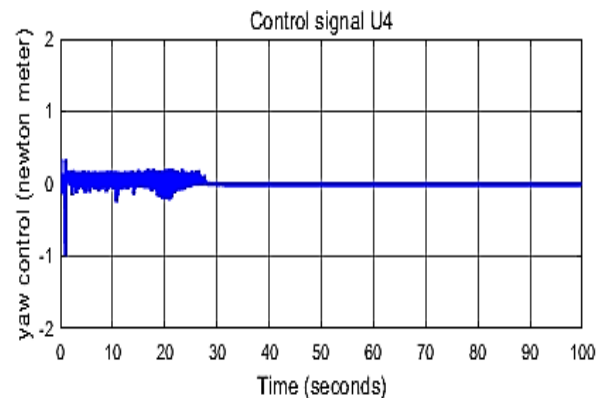


Figure 12. Yaw control signal for tracking



#### F. Higher-order SMC controller performance measure

In this section, the designed higher-order SMC controller performance for tracking is measured in terms of the performance index. Performance indexes are used to measure the controller's effectiveness and accuracy. In this case, the designed controller performance is measured in terms of integral square error (ISE), integral absolute error (IAE), integral time square error (ITSE), integral time absolute error (ITAE), and mean square error (MSE) performance indexes. These indexes' numerical values are tabulated in Table III.

TABLE III. HIGHER-ORDER SMC CONTROLLER PERFORMANCE MEASURE

| Controlled variable | Performance measure indexes |        |          |        |
|---------------------|-----------------------------|--------|----------|--------|
|                     | ISE                         | UAE    | ITS      | MSE    |
| Altitude            | 0.04                        | 0.17   | 0.007495 | 0.017  |
| Pitch               | 0.0001                      | 0.0038 | 0.0006   | 0.0003 |
| Roll                | 0.0002                      | 0.0069 | 0.00017  | 0.0006 |
| Yaw                 | 0.0002                      | 0.0003 | 0.00005  | 0.0003 |

As we have seen from Table 3 that all performance measures numerical values are less than 0.05. This indicates the designed controller is highly effective and accurate in trajectory tracking.

## CONCLUSION

In this paper, the nonlinear dynamic model of the quadrotor is derived using Lagrange formalism. The model contains two parts namely translational and rotational dynamics (Euler-angle dynamics). The nonlinear model includes the gyroscopic moments induced due to the rotational motion of the quadrotor body & propellers mounted on rotor. Besides, the aerodynamic friction moment & force are considered in the modelling. After the derivation of the dynamic model, a nonlinear control strategy (higher-order SMC) based on the supertwisting algorithm has been proposed.

For validating the performance and efficiency of the controller, a simulation is done via Matlab/Simulink. Besides, four performance indexes are implemented to test the effectiveness and accuracy of the designed controller. Second-order SMC is designed for four output-controlled variables separately. The controlled variables are altitude, pitch, roll, and yaw. The second-order SMC was implemented on the physical system for tracking problems. The controller is very effective; it can track the desired trajectory with fast & smooth response and good stability as shown from both simulation and performance index measures. Overall, the second-order SMC controller

designed for the quadrotor for tracking is effective and has excellent performance.

## REFERENCES

- [1] S. Lai, K. Wang, H. Qin, et al., A robust online path planning approach in cluttered environments for micro rotorcraft drones *Control Theory and Technology*, 14(1): 83–96, 2016
- [2] Benić, Z., Piljek, P., and Kotarski, D., 2016, Mathematical modeling of unmanned aerial vehicles with four rotors. *Interdisciplinary Description of Complex Systems* Vol.14, No.1, pp. 88-100.
- [3] Oscar A., 2015, Get Longer Flight Time on Multicopter, web site article <https://oscarliang.com/maximize-flighttime-quadcopter/>
- [4] B. Whitehead and S. Bieniawski. Model Reference Adaptive Control of a Quadrotor UAV. In *Guidance Navigation and Control Conference*
- [5] Samir Bouabdallah, "Design and Control of Quadrotors with Application to Autonomous Flying", MSc thesis Zurich January 2007, DOI: 10.5075/epfl-thesis-3727 · Source: OAI article available at <https://www.researchgate.net/publication/37439805>
- [6] Cen, Z., Noura, H., and Younes, Y.A. (2015). Systematic fault-tolerant control based on adaptive Thau observer estimation for quadrotor UAVs, *International Journal of Applied Mathematics and Computer Science* 25(1): 159–174
- [7] Chenlu, W., Zengqiang, C., Qinglin, S., et al.: 'Design of PID and ADRC based quadrotor helicopter control system,' *Control and Decision Conference (CCDC)*, 2016.
- [8] Merheb, A.-R., Noura, H., and Bateman, F. (2015). Design of passive fault-tolerant controllers of a quadrotor based on sliding mode theory, *International Journal of Applied Mathematics and Computer Science* 25(3): 561–576
- [9] E. I. P. Paul, R. B. Daniel, M. D. Aaron, Stability of small-scale UAV helicopters and quadrotors with an added payload mass under PID control, *Autonomous Robot*, 33: 129–142, 2012.
- [10] R. C. Avram, X. Zhang, and J. Muse, "Nonlinear adaptive fault-tolerant quadrotor altitude and attitude tracking with multiple actuator faults," *IEEE Transactions on Control Systems Technology*, vol. 26, pp. 701–707, March 2018
- [11] S. Mallavalli and A. Fekih, "A fault-tolerant control design for actuator fault mitigation in quadrotor UAVs," in *2019 American Control Conference (ACC)*, pp. 5111–5116, July 2019
- [12] M. E. Antonio-Toledo, E. N. Sanchez, A. Y. Alanis, J. Florez, and M. A. Perez-Cisneros, "Real-time integral backstepping with sliding mode control for a quadrotor UAV," *IFAC-Papers Online*, vol. 51, no. 13, pp. 549–554, 2018. 2nd IFAC Conference on Modelling, Identification, and Control of Nonlinear Systems MICNON 2018.
- [13] Landry, B. (2015). *Planning and control for quadrotor flight* through cluttered environments (Master's Degree Thesis, Massachusetts Institute of Technology).
- [14] Mueller, M. W., Hamer, M., & D'Andrea, R. (2015). Fusing ultra-wideband measurements with accelerometers and rate gyroscopes for quadcopter state estimation. In *2015 IEEE International Conference on Robotics and Automation (ICRA)* (pp. 1730-1736). IEEE
- [15] P. Johan From, J. Tommy Gravdahl, K. Ytterstad Pettersen, *Vehicle Manipulator System*, Verlag, London: Springer, 2014.
- [16] Atheer L. Salih, M. Moghavvemi, Haider A. F. Mohamed, Khalaf Sallom Gaed Modelling, and PID Controller Design for a Quadrotor Unmanned Air Vehicle, *IEEE*, 2010.
- [17] Chenlu, W., Zengqiang, C., Qinglin, S., et al.: 'Design of PID and ADRC based quadrotor helicopter control system,' *Control and Decision Conference (CCDC)*, 2016.
- [18] O. Gherouat, D. Matouk, A. Hassam, and F. Abdessemed, "Modeling and Sliding Mode Control of a Quadrotor Unmanned Aerial Vehicle," *J. Automation and Systems Engineering*, vol. 10, no. 3, pp. 150-157, 2016.
- [19] Landry, B. (2015). *Planning and control for quadrotor flight* through cluttered environments (Master's Degree Thesis, Massachusetts Institute of Technology).
- [20] Samir Bouabdallah, "Design and Control of Quadrotors with Application to Autonomous Flying", MSc thesis Zurich January 2007, DOI: 10.5075/epfl-

thesis-3727. Source: OAI article available at  
<https://www.researchgate.net/publication/37439805>.

#### APPENDICES

Mathematical calculation of control performance index:

$$ISE = \int e^2(t)dt$$

$$IAE = \int |e(t)|dt$$

$$ITSE = \int te^2(t)dt$$

$$MSE = \frac{\int e(t)}{t}$$

